ELSEVIER

Brachytherapy ■ (2013) ■

BRACHYTHERAPY

Dosimetric influence of seed spacers and end-weld thickness for permanent prostate brachytherapy

Christopher S. Melhus[1], Justin K. Mikell[2], Steven J. Frank[3], Firas Mourtada[4,5], Mark J. Rivard[1,*]

[1]*Department of Radiation Oncology, Tufts University School of Medicine, Boston, MA*
[2]*Department of Imaging Physics, The University of Texas MD Anderson Cancer Center, Houston, TX*
[3]*Department of Radiation Oncology, The University of Texas MD Anderson Cancer Center, Houston, TX*
[4]*Department of Radiation Physics, The University of Texas MD Anderson Cancer Center, Houston, TX*
[5]*Department of Radiation Oncology, Christiana Care Hospital, Newark, DE*

ABSTRACT

PURPOSE: The aim of this study was to analyze the dosimetric influence of conventional spacers and a cobalt chloride complex contrast (C4) agent, a novel marker for MRI that can also serve as a seed spacer, adjacent to ^{103}Pd, ^{125}I, and ^{131}Cs sources for permanent prostate brachytherapy.

METHODS AND MATERIALS: Monte Carlo methods for radiation transport were used to estimate the dosimetric influence of brachytherapy end-weld thicknesses and spacers near the three sources. Single-source assessments and volumetric conditions simulating prior patient treatments were computed. Volume−dose distributions were imported to a treatment planning system for dose−volume histogram analyses.

RESULTS: Single-source assessment revealed that brachytherapy spacers primarily attenuated the dose distribution along the source long axis. The magnitude of the attenuation at 1 cm on the long axis ranged from −10% to −5% for conventional spacers and approximately −2% for C4 spacers, with the largest attenuation for ^{103}Pd. Spacer perturbation of dose distributions was less than manufacturing tolerances for brachytherapy sources as gleaned by an analysis of end-weld thicknesses. Volumetric Monte Carlo assessment demonstrated that TG-43 techniques overestimated calculated doses by approximately 2%. Specific dose−volume histogram metrics for prostate implants were not perturbed by inclusion of conventional or C4 spacers in clinical models.

CONCLUSIONS: Dosimetric perturbations of single-seed dose distributions by brachytherapy spacers exceeded 10% along the source long axes adjacent to the spacers. However, no dosimetric impact on volumetric parameters was noted for brachytherapy spacers adjacent to ^{103}Pd, ^{125}I, or ^{131}Cs sources in the context of permanent prostate brachytherapy implants.

Keywords: Seed spacer; Prostate brachytherapy; Dose perturbation; Monte Carlo

Introduction

Low-dose-rate permanent implant brachytherapy is a standard of care approach for the treatment of localized prostate cancer and is delivered to an estimated 40,000 men in the United States each year. Implants typically involve insertion of up to 120 radioactive seeds into the prostate; dosimetric analysis after the implant is critical for evaluating the quality of treatment delivery and is predictive of biochemical disease outcomes after prostate brachytherapy (1). CT is superior to MRI for seed localization, whereas MRI is superior to CT for the anatomic delineation of the prostate and the surrounding soft tissues (2−5). During MRI of the prostate after the implantation, the titanium seeds appear as negative contrast signal voids with susceptibility artifacts. Current MRI sequence protocols make it difficult to localize each seed implanted into the prostate and periprostatic tissues and perform postimplant dosimetric analysis.

Precise dosimetric evaluation of prostate implants is crucial for assessing the adequacy of the treatment

Received 21 May 2013; received in revised form 7 September 2013; accepted 11 September 2013.

Conflict of interest: SJF is a cofounder of C4 Imaging, LLC. All other authors declare no conflicts of interest.

* Corresponding author. Department of Radiation Oncology, Tufts Medical Center, 800 Washington Street, Boston, MA 02111. Tel.: +1 617 636 1680; fax: +1 617 636 7621.

E-mail address: mark.j.rivard@gmail.com (M.J. Rivard).

1538-4721/$ - see front matter
http://dx.doi.org/10.1016/j.brachy.2013.09.004

delivered and thus for ensuring the highest probability of cure. Therefore, current brachytherapy guidelines recently published by the American College of Radiology and the American Brachytherapy Society recommend the fusion of MRI with CT for postimplant dosimetry (6, 7). However, the inadequacies of MRI−CT fusion registration have led to active investigations of seed localization using MRI only (8−12).

To facilitate seed localization by MRI, a cobalt chloride complex contrast (C4) agent was developed that generates a positive signal under MRI (13). The C4 solution is embedded within a polymer capsule of dimensions identical to those of standard seed spacers and placed adjacently to a seed within a strand to enable seed localization under MRI (13). A previous study showed that the dose anisotropy of a single ^{125}I seed was unaffected by the C4 MRI marker and that subsequent imaging of the C4 MRI marker was unaffected by high-dose radiation exposure (14). However, the volumetric dosimetric effects of C4 MRI markers in a standard brachytherapy implant are unknown. Hence, the purpose of this study was to analyze the volumetric dosimetric impact of C4 MRI markers/spacers and conventional markers adjacent to ^{103}Pd, ^{125}I, and ^{131}Cs sources in the context of permanent prostate brachytherapy. Dose perturbations by spacers surrounding a single seed are also presented and compared with dose perturbations based on variations in seed design end-weld thicknesses.

Methods and materials

Monte Carlo (MC) simulations were performed using v1.40 of the MCNP5 radiation transport code. Three different low-energy photon-emitting radionuclide sources were examined: ^{103}Pd model 200 (Theragenics Corporation, Buford, GA), ^{125}I model 6711 (GE Healthcare, Chalfont St. Giles, UK [a unit of General Electric Company]), and ^{131}Cs model CS-1 Rev2 (IsoRay Medical, Inc., Richland, WA). Standard source component configurations and material compositions have been described and benchmarked elsewhere (15).

Three different brachytherapy source spacers were evaluated: ‘‘conventional,’’ C4, and C40 spacers. Conventional spacers were simulated using a 90%/10% molar concentrations of polyglycolic acid/poly L-lactic acid ($C_2H_2O_2$/CH_3O_2) having a mass density of 1.5 g/cm^3. To our knowledge, there are no other spacer types available. C4 spacers consisted of a polyether ether ketone shell ($C_{19}H_{12}O_3$; 1.32 g/cm^3) surrounding a C4 $(CoCl_2)_{0.8}(C_2H_5NO_2)_{0.2}$ (1.01 g/cm^3; Fig. 1) (13, 16). As patients have not yet been implanted with the C4 spacers, consideration for the influence on a higher contrast loading was examined. Specifically, spacers having a C4 agent loading 10 times higher were labeled as C40. These hypothetical C40 spacers were identical to the C4 spacers except that the cobalt chloride complex density was increased to 1.10 g/cm^3. The spacer lengths and diameters were modeled as 0.55 cm and 0.08 cm, respectively.

Photon energies and intensities for each radionuclide source were simulated using data from the U.S. National Nuclear Data Center (17). The MCPLIB04 photon cross-section library DLC-220 was applied for photon-only radiation transport calculations. Owing to the short range of secondary charged particles, energy fluence kerma tallies were used to estimate absorbed dose (*F4). The *F4 tally estimator output (mega electron volts per square centimeter) was converted to absorbed dose (mega electron volts per grams) using mass energy absorption coefficients μ_{en}/ρ (square centimeters per gram) (18). Two simulation geometries were designed to examine volumetric dose distributions: (*1*) single-source simulations showing the influence of adjacent spacers and manufacturing variations and (*2*) multiple source implants simulating clinical cases as described in the following sections.

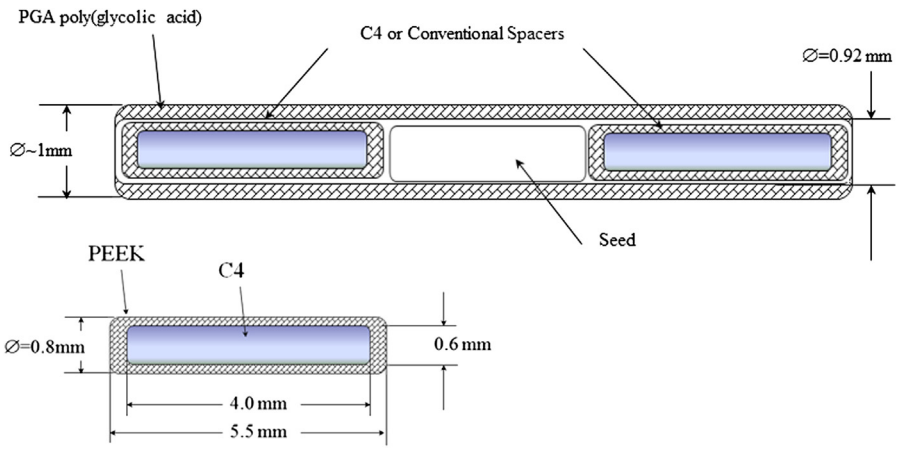

Fig. 1. Schematic representation of a seed with adjacent C4 spacers (MRI markers) as simulated using MC methods for radiation transport simulations. C4 detail illustrates the spacer composition and dimensions. C4 = cobalt chloride complex contrast; MC = Monte Carlo; PEEK = polyether ether ketone.

Single-source simulations

Single-source dose distributions were modeled with a brachytherapy source and spacers aligned along the source long axis in a 15-cm radius homogeneous liquid water phantom. The four simulation geometries included a lone source, a source with conventional spacers, a source with C4 spacers, and a source with C40 spacers. All the three source types were examined. An MC tally was designed to obtain dose distributions in a cylindrical geometry (with the FMESH card), symmetric about the Z-axis (on the $X-Y$ plane) using $(0.01\ \text{mm})^2$ cross-sectional tori for $0 \leq X, Z \leq 2$ cm, where X represents the radial distance from the long axis and Z indicates the distance away from the source center along the source long axis. A separate tally used tori of $(0.05\ \text{mm})^2$ in cross-section for $0 \leq X, Z \leq 10$ cm. A total of 10^9 photon histories were simulated to achieve statistical uncertainties ($k = 1$) less than 0.1% at the reference point (1 cm distance on the source transverse plane) and 3.5% at 2 cm distance on the long axis for the $(0.01\ \text{mm})^2$ toroidal voxels.

To further examine the dosimetric influence of spacers, the source models were varied to increase the thickness of the end welds. Standard source end-weld thicknesses were doubled for each of the three source models in the four spacer-simulation geometries (lone source, source with conventional spacers, source with C4 spacers, and source with C40 spacers). Specifically, dose distributions were calculated to obtain data at 0.1-mm resolution in along and away format for both the nominal end-weld thicknesses of 40, 370, and 76 μm for ^{103}Pd, ^{125}I, and ^{131}Cs, respectively, and for increasing these thicknesses to 80, 560, and 152 μm, respectively. These variations were chosen to approximate those occurring within manufacturer tolerances. Dose distributions in the vicinity of these single seeds also included spacers (conventional, C4, and C40) placed adjacent to the seeds on the long axis.

Clinical implant simulations

To assess the potential influence of the three types of spacers in a simulation of a clinical prostate implant setting, treatment plans from four patients who had received permanent prostate brachytherapy at The University of Texas MD Anderson Cancer Center were selected. These four cases represent typical clinical loading patterns for ^{103}Pd-, ^{125}I-, and ^{131}Cs-bearing implants in large or small prostate volumes (Table 1). In each case, a Day 0 CT scan was obtained immediately after source implantation, and the contours of the prostate, bladder, rectum, and urethra were delineated on the scans. Contrast was not used for the small-prostate ^{103}Pd case, so the urethra was not contoured in that case. For the purposes of this study, the source:spacer modified peripheral loading patterns for ^{125}I and ^{131}Cs were taken to be identical, but the ^{103}Pd loading patterns incorporated a modified uniform loading technique.

Dosimetric information from the Day 0 CT scans was exported from v8.0 of the VariSeed (Varian Medical Systems, Inc., Palo Alto, CA) treatment planning system and imported into v8.8 of the BrachyVision (Varian Medical Systems, Inc.) treatment delivery system. The clinical pretreatment plan was used to group the sources identified on the posttreatment plan according to needle, which provided the relative coordinates of sources and spacers in the implant. To simplify the MC input geometry, the clinical source distribution was modified such that the X (left−right) and Y (anterior−posterior) coordinates of sources in a common needle were set to the average X and Y position of all sources in that needle. For needles with consecutive spacers, the Z (superior−inferior) positions were changed to linearly accommodate the source:spacer sequence as needed, with a maximum source position shift of 0.4 cm (typically <0.1 cm).

Linear source:spacer distributions were constructed by explicitly modeling each source and spacer and then copying and translating them (with TRCL cards) throughout a uniform homogeneous water phantom. A 15-cm radius phantom was used to simulate the scatter conditions for a clinical implant. Three spacer-simulation geometries were created for each case using the data from Table 1: brachytherapy sources with no spacers, brachytherapy sources with conventional spacers, and brachytherapy sources with C4 and conventional spacers, as would be used clinically. For implants using C4 spacers, only spacers adjacent to brachytherapy sources need be C4 spacers. For example, a source−spacer−spacer−spacer−source−source sequence would consist of source−C4 spacer−conventional spacer−C4 spacer−source−source.

Table 1
Characteristics of the four clinical cases analyzed

Prostate size and implant type				
Characteristics	Large prostate, ^{125}I or ^{131}Cs implant	Large prostate, ^{103}Pd implant	Small prostate, ^{125}I or ^{131}Cs implant	Small prostate, ^{103}Pd implant
Prostate volume (cm^3)	63.75	45.34	9.98	14.89
Number of sources	126	128	38	50
Number of spacers	118	126	34	34
Number of C4 spacers	96	102	28	32
Number of needles	30	30	14	16

C4 = cobalt chloride complex contrast.

The geometry of rectilinear output tally volumes was designed (with the FMESH card) to match the brachytherapy dosimetry grids, which used (0.5 mm)^3 cubic voxels. A conversion factor was generated for the tally results to convert *F4 output (square centimeters per gram) to gray for a permanent implant as described by Melhus and Rivard (15). The converted volumetric tally output was subsequently converted to DICOM RTDOSE files using the v8.1 IDL 1 (ITT Exelis, Inc., McLean, VA) software. The RTDOSE files were imported into BrachyVision (Varian Medical Systems, Inc.) to calculate the clinical dosimetric parameters recommended by the American Brachytherapy Society and the American Association of Physicists in Medicine (AAPM) TG-137 report (7, 19), namely D_{90}, D_{100}, V_{90}, V_{100}, V_{150}, and V_{200} for the prostate; $D_{0.1\ cm^3}$, $D_{1\ cm^3}$, and $D_{2\ cm^3}$ for the bladder and rectum; and $D_{0.1\ cm^3}$, D_5, D_{10}, and D_{30} for the urethra.

In addition to MC calculations, conventional brachytherapy dosimetry calculations based on the AAPM TG-43U1 report (20) were performed using the linear source approximation for ^{103}Pd, ^{125}I, and ^{131}Cs sources based on the published dosimetry parameters. The source data used for models 200 ^{103}Pd and 6711 ^{125}I were obtained from the AAPM TG-43U1 report consensus data (20), and the model CS-1 Rev2 ^{131}Cs source dosimetry parameters were obtained from the study by Rivard (21, 22).

A total of 10^9 starting particles were simulated for ^{103}Pd source and 5×10^8 particles for ^{125}I and ^{131}Cs sources to achieve statistical uncertainties ($k = 1$) <3% throughout the simulation volume. For example, the bladder dose in the large prostate cases had mean statistical uncertainties of 2.8% (maximum, 6.5%), 2.3% (maximum, 8.3%), and 1.6% (maximum, 3.4%) for ^{103}Pd, ^{125}I, and ^{131}Cs, respectively. The mean statistical uncertainties in the prostate volume were lower because of the smaller distance between the sources and the organ and were 0.9% (maximum, 1.2%), 1.1% (maximum, 1.5%), and 0.8% (maximum, 1.2%) for ^{103}Pd, ^{125}I, and ^{131}Cs, respectively.

Results

Dosimetric influence of source spacers

MC simulations of individual model 200 ^{103}Pd, model 6711 ^{125}I, and model CS-1 Rev2 ^{131}Cs sources with adjacent brachytherapy spacers revealed photon attenuation in the spacers; however, most of the volume surrounding the source was not perturbed. As expected, most of the attenuation was along the source long axis, where the path length through the spacer was the longest. Figure 2 illustrates the relative dose between source in homogeneous water and source with adjacent spacer in homogeneous water within a Cartesian plane with ($X = 0$ cm and $Y = 0$ cm), representing the center of the source for ^{103}Pd (top panels) and ^{125}I (bottom panels). Results for the ^{125}I sources were similar to ^{131}Cs (data not shown).

As expected, the dose distribution was perturbed less with the higher energy ^{125}I and ^{131}Cs sources because of less absorption by the spacers. The relative dose decrease on the long axis at ($X = 0$ cm and $Z = 1$ cm) for each source and all three spacer materials is shown in Table 2. The hypothetical C40 spacer (with a 10 times higher agent concentration) demonstrated the largest attenuation along the source long axis; photon attenuation in the C4 spacer was less than that of the conventional seed spacers. Although it had a higher mean photon energy, dosimetric influence of source spacers was higher for the ^{131}Cs seed than that for the ^{125}I seed. This is thought to be because of the larger solid angle subtended by the spacer for the ^{131}Cs seed and subsequently smaller proportion of primary dose in comparison with the ^{125}I seed, which has radioactivity distributed on the surfaces of a radiopaque marker.

Dosimetric influence of end-weld thickness

The model 200 ^{103}Pd source showed the most variation in dose distribution as a function of end-weld thickness. This is because photons emitted from active components may attenuate through two thickened source capsule components because of the concave end-weld geometry. Furthermore, the average photon energy emitted by ^{103}Pd is 21 keV compared with an average of approximately 30 keV for ^{125}I and ^{131}Cs sources.

Comparing dose distributions for the model 200 ^{103}Pd with adjacent C4 spacer (Fig. 3, left), the ratio is within ±1% of unity within ±35° of the transverse plane, up to +5% of unity within ±58° of the transverse plane, up to +10% of unity within ±67° of the transverse plane, and up to +20% of unity within ±78° of the transverse plane. The ratio deviated from unity by up to 30% on the source long axis. Similar results were obtained for the conventional spacer and the C40 spacer, demonstrating that end-weld perturbations of dose distributions were independent of spacer design.

For the model CS-1 Rev2 ^{131}Cs brachytherapy source and C4 spacer, end-weld thickness variations resulted in dose distribution variations approaching 20% at close distances on the source long axis (Fig. 3, right). The ratio was within ±1% of unity within ±52° of the transverse plane, within +1%−+3% of unity within ±73° of the transverse plane, and within +3%−+5% of unity within ±81° of the seed transverse plane. Thus, dose differences exceeding 5% occurred only at relatively small solid angles along the source long axis. As was true for ^{103}Pd, the dose distributions for ^{131}Cs were similarly perturbed for the conventional and C40 spacers. The model 6711 ^{125}I source provided results similar to those for the model CS-1 Rev2 ^{131}Cs.

Clinical implant simulations

MC simulations comparing the dosimetric influence on dose−volume histogram (DVH) parameters for all

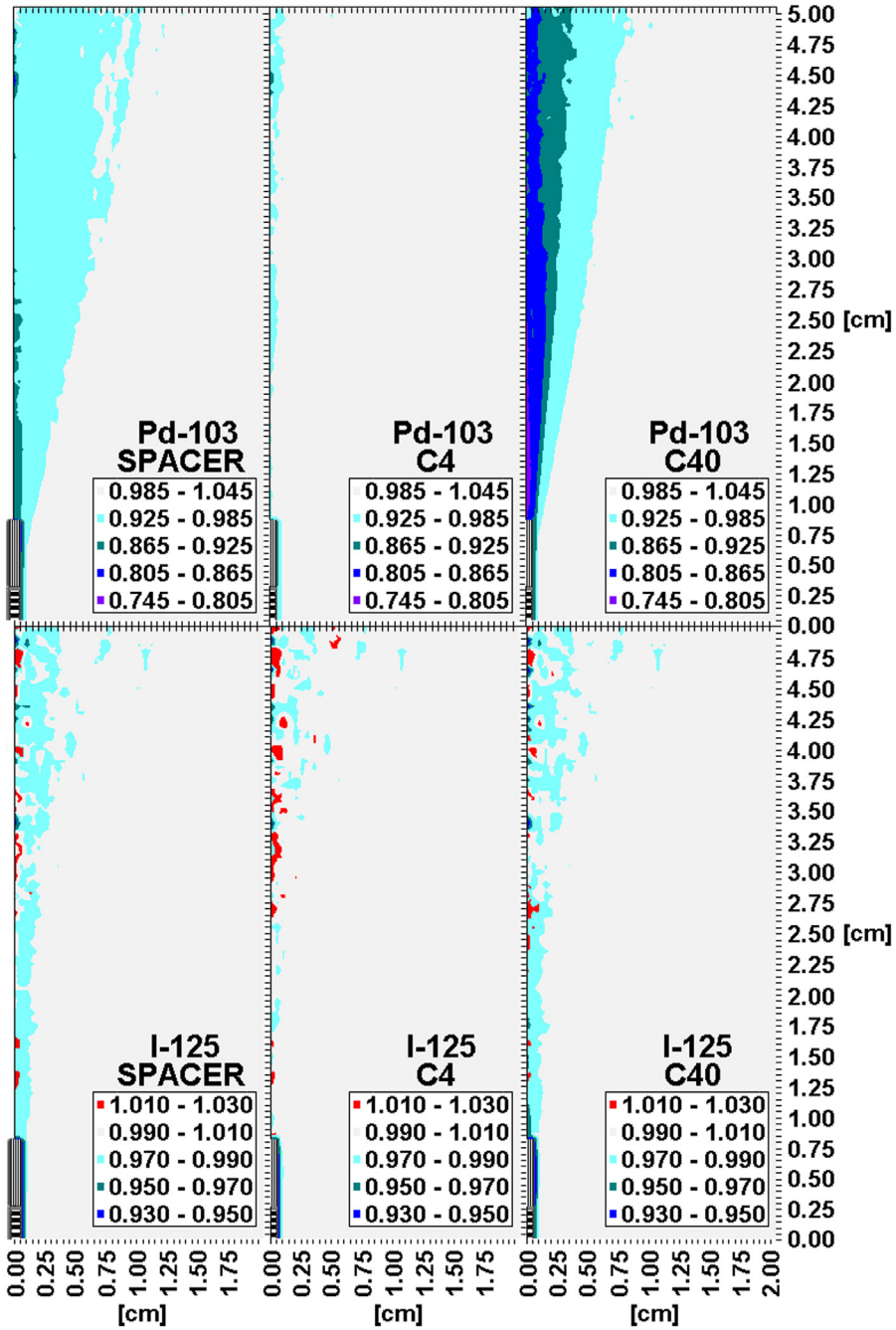

Fig. 2. The relative dose distributions for ^{103}Pd (upper panels, with 3% bin width) and ^{125}I (lower panels, with 2% bin width) for a source in homogeneous water and a source with adjacent spacer for the model 6711 ^{125}I source and three different spacers. In the lower left corner of each panel, the bold horizontal striped object represents the upper half of the source, and the vertically striped object represents the spacer.

the three radionuclides using either conventional or C4 spacers relative to using no spacers, that is, water is the medium between the seeds, indicated perturbation of DVH parameters by <0.3% for the large prostates and 0.6% for the small prostates. All these prostate DVH perturbations were less than the mean statistical uncertainties. Thus, the examined volumetric dose perturbations by the seeds were not statistically significant within 1%.

DVH parameters calculated using MC simulations with conventional and C4 spacers vs. the conventional TG-43 dose formalism (intrinsically without accounting for inter-seed attenuation or spacers) revealed perturbations within 5% except for the large prostate loaded with ^{131}Cs seeds. For the conventional and C4 spacers, the MC-calculated V_{150} was −10% and the V_{200} was −6% compared with what was found using the TG-43 approach. The maximum statistical ($k = 1$) uncertainties within the prostate volumes

Table 2
Relative dose decreases in water at a distance of 1 cm along the long axis, that is, $Z = 1$ cm, integrated over $0 \leq X \leq 0.075$ cm for the three sources and three spacer materials

Source model and radionuclide	Conventional	Spacers C4	C40
200 ^{103}Pd	0.925	0.989	0.822
6711 ^{125}I	0.979	0.996	0.977
CS-1 Rev2 ^{131}Cs	0.962	0.993	0.936

C4 = cobalt chloride complex contrast.

The values provided did not change by more than 1% for $Z = 2$ cm. The $k = 1$ statistical uncertainties for the dose ratios of spacer to no spacer were uniformly 0.3%.

were 1.5% for all three source models—smaller than the observed differences in the DVH parameters. Collectively, these results indicate no meaningful differences in terms of dosimetric impact on organs at risk and target coverage for the conventional spacer, C4 spacer, or for no spacer altogether.

Discussion

To our knowledge, this is the first analysis of the influence of spacers adjacent to radioactive seeds on volumetric dosimetry in prostate brachytherapy. Evaluation of the influence of source spacers demonstrated that photon attenuation in the C4 spacer was less than that caused by conventional brachytherapy spacers, and the attenuation was highest for the hypothetical C40 spacer. The relative differences in dose distributions of the seeds with adjacent C4 spacers were not perturbed by variations in end-weld thickness of the ^{103}Pd, ^{125}I, and ^{131}Cs seeds. However, the magnitude of the relative differences illustrated that manufacturing tolerances could generate source-specific dose perturbations that exceed those introduced by the presence of source spacers.

Spacers are commonly used in prostate brachytherapy and are typically placed adjacent to the radioactive sources within strands. The C4 spacer was developed to enable localization of the implanted seeds under MRI alone to allow a more accurate assessment of postimplant dosimetry than that provided by CT (14). The C4 spacer can be visualized using T1- and T2-weighted MRI protocol sequences, which can improve the ability to identify soft tissues in the postimplant setting over CT. A recent study demonstrated both the safety of the C4 solution and the *in vivo* visualization of the C4 spacers within a strand in a canine prostate (16). As noted previously, accurate assessment of postimplant dosimetry is critical for quality assurance. If an implant is determined to be dosimetrically inadequate, additional seeds can be placed to improve it. Conversely, if postimplant dosimetry identifies excessive doses to adjacent critical structures, potential toxicities can be anticipated and prophylactic conservative management discussed with the patient and initiated. Optimal assessment of postimplant dosimetry can also help the brachytherapy team to improve their techniques to facilitate consistency within the program.

Conclusions

Assessment of single-seed dose distributions revealed that the dosimetric perturbations of the brachytherapy spacers exceeded 10% at positions located along the source long axes immediately adjacent to the spacers. However, no observable dosimetric impact on volumetric parameters was noted for brachytherapy spacers adjacent to ^{103}Pd, ^{125}I, or ^{131}Cs sources in the context of permanent prostate brachytherapy implants. Indeed, the dosimetric impact of the spacers was shown to be smaller than variations in source end-weld thickness intrinsic to the manufacturing process. We conclude that the practice of excluding the dosimetric influence of brachytherapy spacers from radiation therapy calculations in permanent volumetric implants

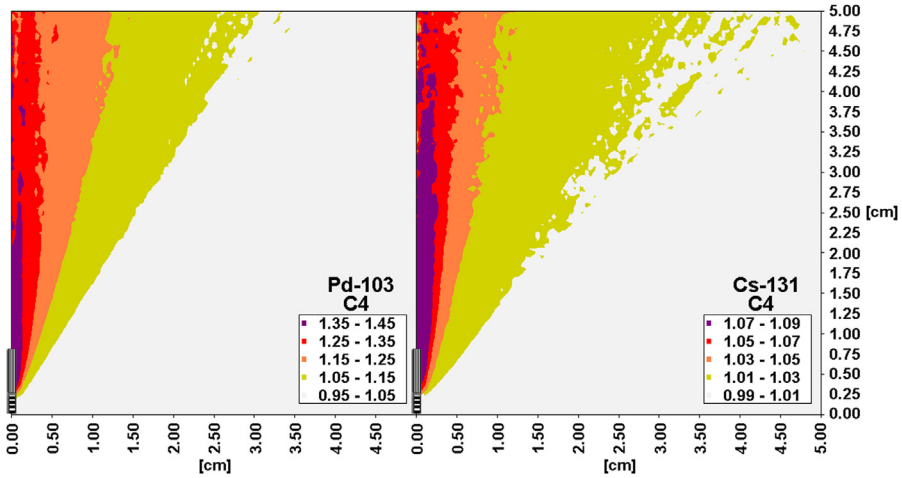

Fig. 3. Ratio of relative dose distributions for the model 200 ^{103}Pd source (left) and CS-1 Rev2 ^{131}Cs source (right) with two different end-weld thicknesses and adjacent C4 spacers. C4 = cobalt chloride complex contrast.

does not change the examined volumetric parameters within 1%.

Acknowledgments

The authors thank Teresa L. Bruno, Medical Dosimetrist, at MD Anderson Cancer Center, for her help with this project.

References

[1] Stock RG, Stone NN. Importance of post-implant dosimetry in permanent prostate brachytherapy. *Eur Urol* 2002;41:434−439.

[2] Rasch C, Barillot I, Remeijer P, *et al*. Definition of the prostate in CT and MRI: A multi-observer study. *Int J Radiat Oncol Biol Phys* 1999; 43:57−66.

[3] Amdur RJ, Gladstone D, Leopold KA, *et al*. Prostate seed implant quality assessment using MR and CT image fusion. *Int J Radiat Oncol Biol Phys* 1999;43:67−72.

[4] Crook J, McLean M, Yeung I, *et al*. MRI-CT fusion to assess postbrachytherapy prostate volume and the effects of prolonged edema on dosimetry following transperineal interstitial permanent prostate brachytherapy. *Brachytherapy* 2004;3:55−60.

[5] Albert JM, Swanson DA, Pugh TJ, *et al*. Magnetic resonance imaging-based treatment planning for prostate brachytherapy. *Brachytherapy* 2013;12:30−37.

[6] Frank SJ, Arterbery VE, Hsu IC, *et al*. American College of Radiology appropriateness criteria permanent source brachytherapy for prostate cancer. *Brachytherapy* 2011;10:357−362.

[7] Davis BJ, Horwitz EM, Lee WR, *et al*. American Brachytherapy Society consensus guidelines for transrectal ultrasound-guided permanent prostate brachytherapy. *Brachytherapy* 2012;11:6−19.

[8] Kuo N, Lee J, Tempany C, *et al*. MRI-based prostate brachytherapy seed localization. *Proceedings IEEE Int Symp Biomed Imaging* 2010; 2010:1397−1400.

[9] Lee RJ, Suh HS, Lee KJ, *et al*. A magnetic resonance-based seed localization method for I-125 prostate implants. *J Korean Med Sci* 2007;22:S129−S133.

[10] Ohashi T, Momma T, Yamashita S, *et al*. Impact of MRI-based postimplant dosimetric assessment in prostate brachytherapy using contrast-enhanced T1-weighted images. *Brachytherapy* 2012;11: 468−475.

[11] Bloch BN, Lenkinski RE, Helbich TH, *et al*. Prostate postbrachytherapy seed distribution: Comparison of high-resolution, contrast-enhanced, T1- and T2-weighted endorectal magnetic resonance imaging versus computed tomography: initial experience. *Int J Radiat Oncol Biol Phys* 2007;69:70−78.

[12] Thomas SD, Wachowicz K, Fallone BG. MRI of prostate brachytherapy seeds at high field: A study in phantom. *Med Phys* 2009;36: 5228−5234.

[13] Frank SJ, Stafford RJ, Bankson JA, *et al*. A novel MRI marker for prostate brachytherapy. *Int J Radiat Oncol Biol Phys* 2008;71:5−8.

[14] Frank SJ, Tailor RC, Kudchadker RJ, *et al*. Anisotropy characterization of I-125 seed with attached encapsulated cobalt chloride complex contrast agent markers for MRI-based prostate brachytherapy. *Med Dosim* 2010;36:200−205.

[15] Melhus CS, Rivard MJ. COMS eye plaque brachytherapy dosimetry simulations for ^{103}Pd, ^{125}I, and ^{131}Cs. *Med Phys* 2008;35: 3364−3371.

[16] Frank SJ, Johansen MJ, Martirosyan KS, *et al*. A biodistribution and toxicity of cobalt dichloride-N-acetyl cysteine in an implantable MRI marker for prostate cancer treatment. *Int J Radiat Oncol Biol Phys* 2013;85:1024−1030.

[17] NUDAT 2.6. National Nuclear Data Center. Brookhaven National Laboratory. Available at: http://www.nndc.bnl.gov/nudat2/index.jsp. Accessed September 4, 2013.

[18] Hubbell JH, Seltzer SM. *Tables of X-ray mass attenuation coefficients and mass energy-absorption coefficients (version 1.4)*. Gaithersburg, MD: National Institute of Standards and Technology; 2004. [Online] Available at: http://physics.nist.gov/xaamdi. Accessed September 4, 2013.

[19] Nath R, Bice WS, Butler WM, *et al*. AAPM recommendations on dose prescription and reporting methods for permanent interstitial brachytherapy for prostate cancer: Report of Task Group 137. *Med Phys* 2009;36:3510−3522.

[20] Rivard MJ, Coursey BM, DeWerd LA, *et al*. Update of AAPM Task Group No. 43 Report: A revised AAPM protocol for brachytherapy dose calculations. *Med Phys* 2004;61:633−674.

[21] Rivard MJ. Brachytherapy dosimetry parameters calculated for a ^{131}Cs source. *Med Phys* 2007;34:754−762.

[22] Rivard MJ. Erratum: "Brachytherapy dosimetry parameters calculated for a ^{131}Cs source. [Med Phys 2009;36:279]". *Med Phys* 2007;34:754−762.